PHYSICAL REVIEW FLUIDS **1**, 084502 (2016)

Linearized propulsion theory of flapping airfoils revisited

R. Fernandez-Feria
Universidad de Málaga, Andalucía Tech, E. T. S. Ingeniería Industrial, Dr Ortiz Ramos s/n, 29071 Málaga, Spain
(Received 4 July 2016; published 27 December 2016)

A vortical impulse theory is used to compute the thrust force of a plunging and pitching airfoil in forward flight at high Reynolds numbers within the framework of linear potential flow theory. The result is significantly different from the classical one of Garrick, which considered only two effects, the leading-edge suction and the projection in the flight direction of the pressure force on the airfoil. By taking into account the complete vorticity distribution on the airfoil and the wake the mean thrust coefficient contains, in addition to the pressure force projection term, a new term that generalizes the leading-edge suction term in Garrick's theory. This term depends on Theodorsen function $C(k)$ and on a new complex function $C_1(k)$ of the reduced frequency k. The main qualitative difference with Garrick's theory is that the propulsive efficiency, or ratio of the mean thrust power and the mean input power required to drive the airfoil, tends to zero as the reduced frequency increases to infinity (as k^{-1}), in contrast to Garrick's propulsive efficiency that tends to a constant (1/2). Consequently, for pure pitching and combined pitching and plunging motions, the maximum of the propulsive efficiency is not reached as $k \to \infty$ like in Garrick's theory, but at a finite value of the reduced frequency that depends on the remaining nondimensional parameters. The present analytical results are in good agreement, for small amplitude oscillations, with numerical results from unsteady panel methods, and with experimental data and numerical results from the Navier-Stokes equations, except for small reduced frequencies where viscous effects are obviously important.

DOI: 10.1103/PhysRevFluids.1.084502

I. INTRODUCTION

Unsteady aerodynamics of flapping airfoils is now a subject of active research because of the recent interest in the development of microaerial vehicles, bioinspired by small flying animals [1,2]. But it has a long tradition starting from the early 20th century. In particular, Glauert [3] and Theodorsen [4] developed theoretical analyses for the force and moment on oscillating airfoils in forward flight at high Reynolds numbers within the framework of linear, two-dimensional potential flow theory. Taking into account the unsteady vorticity wake, Theodorsen [4] obtained analytical relations for the lift and moment of pitching and plunging airfoils which were subsequently rationalized by von Kármán and Sears [5], decomposing them into three distinct physical contributions: the quasisteady lift and moment generated by the bound circulation, the apparent mass contribution, and the contribution from the wake vorticity. In this linear potential theory it is assumed an inviscid flow and small amplitude oscillations of the airfoil, with a horizontal plane wake in first approximation. Following a method stated by von Kármán and Burgers [6], Garrick [7] extended Theodorsen's work to obtain also the thrust of a pitching and plunging airfoil by considering only two contributions, the leading-edge suction due to the high-speed flow about the leading edge and the projection in the flight direction of the pressure force on the airfoil. This propulsion linear theory overestimates the time-averaged propulsion coefficient and propulsive efficiency for small amplitude oscillations, not only for small frequencies, where obviously viscous effects cannot be neglected, but also for intermediate and high frequencies of the oscillations [8–12]. The main aim of the present paper is to correct these deficiencies by deriving the thrust force within the linear potential flow framework by using a more general vortical impulse theory.

To be more specific, von Kármán and Sears [5] developed general expressions for the lift and moment using the theorem of moment of momentum conservation, or impulse theory, which for an oscillating airfoil reproduced previous results by Theodorsen [4] based on velocity potentials for the circulatory and noncirculatory flows. Both approaches are equivalent because they are based on the correct computation of the vorticity distribution generated by the unsteady vortex wake and on the Kutta condition at the trailing edge. Garrick [7] used Theodorsen's results for the velocity potentials and for the lift force to compute the projection of the pressure force and the leading-edge suction force, which were used to obtain the thrust or propulsion force. But this force in the flight direction can be computed, like the lift force, in a more general way by using the vortical impulse theory developed later by Lighthill and Saffman, among others (see, e.g., Refs. [13–15]). Thus, the general vortical impulse theory is used in the present paper to compute the thrust or drag force of a plunging and pitching airfoil, generalizing Garrick's propulsion based on Theodorsen results (T-G propulsion theory for short) but which considered only, in addition to the projection of the pressure force, the leading-edge suction force. By using the same wake vorticity first obtained by Theodorsen [4] to compute the lift force, the vortical impulse theory takes into account its effect all over the airfoil, and not only at the leading-edge, to yield a more accurate analytical expression for the thrust force.

The resulting time-averaged thrust and propulsive efficiency are in general smaller than those predicted by the T-G propulsion theory, particularly for large frequencies, approaching results based on numerical simulations from the full Navier-Stokes equations and experimental data. Of course, the theory still neglects the effect of the leading-edge vortex, which has been proved to be very relevant in the unsteady thrust (and lift) generated by plunging and pitching airfoils [16–24], especially at low Reynolds numbers. But it provides an analytical approximation that, like the classical Theodorsen theory for lift and moment, may be useful to estimate forces on a flapping airfoil, improving the propulsion and propulsive efficiency predicted by Garrick's theory. The effect of the leading-edge vortex, or of additional leading or trailing edge vortices, may be latter included in the formulation as done, for instance, in the recent work by Li and Wu [25] for the Wagner's problem [26], which is also a linearized theory but for a suddenly starting flat plate.

The general unsteady aerodynamic problem is formulated in Sec. II, including a summary of some of the results by Theodorsen [4], Garrick [7], and von Kármán and Sears [5] needed to evaluate some of the integrals appearing in the new propulsion formulation. Part of this summary is relegated to the appendices, particularly the lift and moment coefficients [4,5] needed to compute the input power required to drive the airfoil and, therefore, the propulsive efficiency. Section III presents the main results on propulsion force and propulsive efficiency, which are compared in Sec. IV with Garrick's results, and with some other numerical and experimental results.

II. FORMULATION OF THE PROBLEM AND SUMMARY OF THEODORSEN LIFT AND MOMENT

We consider the two-dimensional (2D), incompressible, and inviscid flow over a plunging and pitching thin airfoil of chord length c that translates with constant speed U along the x axis (see Fig. 1). The vertical amplitudes of the heaving and pitching motions are both very small compared to c so that the airfoil and every point of the trail of vortices which it leaves behind may be considered to be upon the x axis in first approximation.

For simplicity we take $c = 2$, so that all the lengths are scaled with the half-chord $c/2$ and the airfoil extends from $x = -1$ to $x = 1$, approximately, in a frame translating with it at speed U along the x axis. In this reference frame the motion of the airfoil is given by the vertical displacement (see Fig. 1):

$$z_s(x,t) = h(t) - (x - a)\alpha(t), \quad -1 \leqslant x \leqslant 1 \tag{1}$$

with

$$h(t) = \Re[h_0 e^{i\omega t}], \quad \alpha(t) = \Re[\alpha_0 e^{i\omega t}], \tag{2}$$

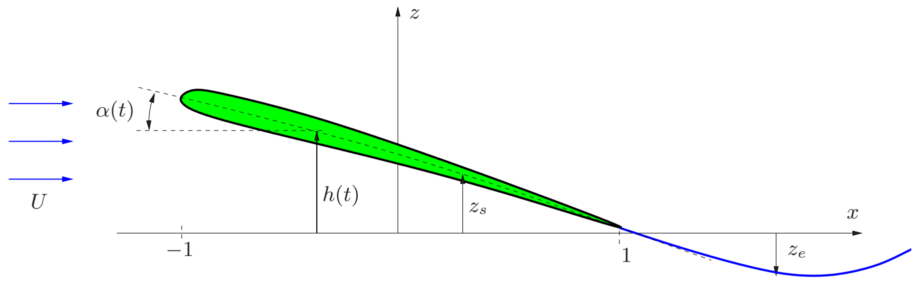

FIG. 1. Schematic of the oscillating airfoil and wake.

where ω is the frequency of the oscillations of both the heaving motion, $h(t)$, and the pitching rotation around the horizontal axis $x = a$ [i.e., the dimensional pivoting distance from the leading-edge is $s_p = (1 + a)c/2$], and $\Re$ means real part. The amplitudes h_0 and α_0 are in general complex constants (to account for any phase shift between both oscillations) satisfying $|h_0| \ll 1$ and $|\alpha_0| \ll 1$. For simplicity we select h_0 real and

$$\alpha_0 = a_0 e^{i\phi}, \tag{3}$$

with ϕ the phase shift between the plunging and pitching motions and a_0 the maximum pitching amplitude. In what follows we shall work with the complex functions knowing that we have to take the real part of the results. The vertical velocity of the rigid airfoil is

$$v_0(x,t) = \dot{h} - (x - a)\dot{\alpha} - U\alpha, \tag{4}$$

where a dot denotes the time derivative.

The vortical impulse theory for an incompressible and unbounded flow is used to obtain the forces on the airfoil. Neglecting the volume (section) of the airfoil, one may write [15]

$$\mathbf{F} \equiv D\mathbf{e}_x + L\mathbf{e}_z = -\rho\frac{d\mathbf{I}}{dt}, \tag{5}$$

where D is the drag (or minus the thrust) force, L is the lift force, both per unit span, ρ the fluid density, and the vortical impulse (or vorticity moment) $\mathbf{I}$ is

$$\mathbf{I} = \int_{\mathcal{V}} \mathbf{x} \wedge \boldsymbol{\omega}\, d\mathcal{V}, \tag{6}$$

where $\boldsymbol{\omega} = \nabla \wedge \mathbf{v}$ is the vorticity field and $\mathcal{V}$ is the entire volume (area in this case) occupied by the fluid plus the airfoil. In writing (5) it is assumed that $\mathcal{V}$ is not only unbounded, but that the flow is potential far from the airfoil [14,15].

In the thin airfoil theory it is assumed that the vorticity, which is directed along the normal $\mathbf{e}_y$ to the plane of the fluid motion, is concentrated at the airfoil surface and at the trailing wake, both considered as vortex sheets. Thus,

$$\mathbf{I} \simeq \int_{-1}^{1} (-z_s\varpi_s\mathbf{e}_x + x\varpi_s\mathbf{e}_z)\, dx + \int_{1}^{\infty} (-z_e\varpi_e\mathbf{e}_x + x\varpi_e\mathbf{e}_z)\, dx, \tag{7}$$

where $\varpi_s(x,t)$, $-1 \leqslant x \leqslant 1$, is the vorticity density distribution on the airfoil, $\varpi_e(x,t)$ is the vorticity density distribution in the trailing wake, and $z_e(x,t)$ is the vertical position of each point in this vortex wake (Fig. 1). It is considered the large-time behavior in which the vortex wake extends many chord lengths downstream of the airfoil, so that, in first approximation, $1 \leqslant x \leqslant \infty$ for both $\varpi_e(x,t)$ and $z_e(x,t)$, with $|z_e| \ll 1$ in the present linearized theory. Consequently, under the assumptions made, the drag and lift forces on the airfoil are given by

$$D = \rho \frac{d}{dt} \int_{-1}^{1} z_s \varpi_s \, dx + \rho \frac{d}{dt} \int_{1}^{\infty} z_e \varpi_e \, dx, \tag{8}$$

$$L = -\rho \frac{d}{dt} \int_{-1}^{1} x \varpi_s \, dx - \rho \frac{d}{dt} \int_{1}^{\infty} x \varpi_e \, dx. \tag{9}$$

On the other hand, the vortical impulse theory also provides the moment on the airfoil,

$$\mathbf{M} = M \mathbf{e}_y = -\rho \frac{d\mathbf{A}}{dt}, \tag{10}$$

where

$$\mathbf{A} = -\frac{1}{2} \int_{\mathcal{V}} |\mathbf{x}|^2 \boldsymbol{\omega} \, d\mathcal{V} \simeq -\frac{1}{2} \mathbf{e}_y \left(\int_{-1}^{1} x^2 \varpi_s \, dx + \int_{1}^{\infty} x^2 \varpi_e \, dx \right) \tag{11}$$

is the angular impulse [14,15].

The lift (L) and moment (M) for an oscillating thin airfoil were computed by von Kármán and Sears [5] using (9) and (10), reproducing previous results by Theodorsen [4] but in a more general framework. To that end von Kármán and Sears [5] separated the contribution of the wake to ϖ_s from the bound circulation that would be produced by the motion of the airfoil as if the wake had no effect:

$$\varpi_s(x,t) = \varpi_0(x,t) + \varpi_1(x,t), \quad -1 \leqslant x \leqslant 1, \tag{12}$$

with

$$\int_{-1}^{1} \varpi_0(x,t) \, dx = \Gamma_0(t) \tag{13}$$

the bound circulation, and

$$\varpi_1(x,t) = \frac{1}{\pi} \int_{1}^{\infty} \sqrt{\frac{\xi+1}{\xi-1}} \sqrt{\frac{1-x}{1+x}} \frac{\varpi_e(\xi,t)}{(\xi - x)} \, d\xi, \tag{14}$$

where the Kutta-Joukowski condition is applied at the trailing edge. Applying Kelvin's theorem of vanishing total circulation, they obtained the following general relation between $\varpi_e(x,t)$ and $\Gamma_0(t)$:

$$\Gamma_0(t) + \int_{1}^{\infty} \sqrt{\frac{\xi+1}{\xi-1}} \, \varpi_e(\xi,t) \, d\xi = 0. \tag{15}$$

Then, substituting into (9), von Kármán and Sears obtained the following general relation for the lift:

$$L = L_0 + L_1 + L_2, \tag{16}$$

where

$$L_0 = \rho U \Gamma_0, \quad L_1 = -\rho \frac{d}{dt} \int_{-1}^{1} x \varpi_0 \, dx \quad \text{and} \quad L_2 = \rho U \int_{1}^{\infty} \frac{\varpi_e}{\sqrt{\xi^2 - 1}} \, d\xi \tag{17}$$

are the quasisteady lift, the apparent mass lift, and the wake lift, respectively, and similar general expressions were obtained for the moment M. Finally, by considering the oscillatory motion (1) of the thin airfoil, the following expressions for Γ_0, ϖ_0, and ϖ_e are obtained:

$$\Gamma_0 = 2\pi\left[U\alpha - \dot{h} - \left(a - \frac{1}{2}\right)\dot{\alpha}\right] \equiv G_0 e^{i\omega t}, \quad G_0 = 2\pi[U\alpha_0 - i\omega h_0 - i\omega(a - 1/2)\alpha_0], \tag{18}$$

$$\varpi_0(x,t) = g_0(x)e^{i\omega t}, \quad g_0(x) = \frac{1}{\sqrt{1-x^2}}\left[\frac{G_0}{\pi} + 2(i\omega h_0 + i\omega a\alpha_0 - U\alpha_0)x + i\omega\alpha_0(1 - 2x^2)\right], \tag{19}$$

$$\varpi_e(\xi,t) = g e^{i\omega(t-\xi/U)}, \quad g = -\frac{G_0}{\int_1^\infty \sqrt{\frac{\xi+1}{\xi-1}}\, e^{-i\omega\xi/U} d\xi} = \frac{2G_0}{\pi}\frac{1}{iH_0^{(2)}(k) + H_1^{(2)}(k)}, \tag{20}$$

where $H_n^{(2)}(z) = J_n(z) - iY_n(z)$, $n = 0,1$, are Hankel functions, related to the Bessel functions J_n and Y_n [27], and k is the reduced frequency

$$k = \frac{\omega}{U}. \tag{21}$$

Note that we are taking $c = 2$, so that all the lengths are scaled with $c/2$ and the dimensionless reduced frequency is actually $k = c\omega/(2U)$.

The relation between the integral in Eq. (20) and the Hankel (or Bessel) functions was given by Theodorsen [4], who derived the following relations for the lift and moment of an oscillating thin airfoil using a different approach to that summarized here due to von Kármán and Sears [5]:

$$L = \pi\rho(U\dot{\alpha} - \ddot{h} - a\ddot{\alpha}) + \rho U\Gamma_0 C(k), \tag{22}$$

$$M = -\pi\rho\left[\left(\tfrac{1}{2} - a\right)U\dot{\alpha} + \left(\tfrac{1}{8} + a^2\right)\ddot{\alpha} + a\ddot{h}\right] + \rho U\Gamma_0\left(a + \tfrac{1}{2}\right)C(k), \tag{23}$$

where

$$C(k) = \frac{H_1^{(2)}(k)}{iH_0^{(2)}(k) + H_1^{(2)}(k)} \equiv F(k) + iG(k) \tag{24}$$

is the Theodorsen function [4,28].

The corresponding lift and moment coefficients are summarized in Appendix A.

III. PROPULSION FORCE AND PROPULSIVE EFFICIENCY

Following von Kármán and Burgers [6], Garrick [7] used the linearized theory of Theodorsen [4] for an oscillating airfoil to compute the propulsive (or drag) force by taking into account the projection along the x axis of the lift force normal to the foil and the leading-edge suction force. We shall see that this propulsive force, which is summarized in Appendix B, does not coincide with that obtained from the more general expression (8).

Before substituting (12)–(14) and (1) into (8) it is convenient to note that the expression (20) for ϖ_e comes from the assumption that the vorticity in the wake is convected downstream with velocity U, so that ϖ_e remains constant in a reference frame stationary with the far field fluid, $\varpi_e(\xi,t) = \varpi_e(X)$, with $X = \xi - Ut$ [this property is also used to obtain L_2 in Eq. (17)]. The same can be said for the vertical displacement of the wake, $z_e(\xi,t) = z_e(X)$. In fact, it must coincide with the trailing edge vertical displacement at the time $t' = t + (1-\xi)/U = (1-X)/U$ when it was shed from the airfoil, $z_e(X) = z_s(x = 1,t')$:

$$z_e(X) = h\left(\frac{1-X}{U}\right) - (1-a)\alpha\left(\frac{1-X}{U}\right). \tag{25}$$

Thus,

$$\frac{d}{dt}\int_1^\infty z_e\varpi_e\,d\xi = \frac{d}{dt}\int_{1-Ut}^\infty z_e(X)\varpi_e(X)\,dX = U[h(t)-(1-a)\alpha(t)]\varpi_e(\xi=1,t). \tag{26}$$

Taking into account that

$$\begin{aligned}\frac{d}{dt}\int_{-1}^1 \varpi_1\,dx &= \frac{d}{dt}\int_1^\infty\left(\frac{\sqrt{\xi+1}}{\sqrt{\xi-1}}-1\right)\varpi_e\,d\xi = -\frac{d}{dt}\left(\Gamma_0+\int_1^\infty \varpi_e\,d\xi\right)\\ &= -\frac{d\Gamma_0}{dt} - U\varpi_e(\xi=1,t),\end{aligned} \tag{27}$$

$$\frac{d}{dt}\int_{-1}^1 x\varpi_1\,dx = \frac{d}{dt}\int_1^\infty(\sqrt{\xi^2-1}-\xi)\varpi_e\,d\xi = U\int_1^\infty \frac{\xi}{\sqrt{\xi^2-1}}\varpi_e\,d\xi - U\int_1^\infty \varpi_e\,d\xi, \tag{28}$$

and using the total-circulation conservation (15) [which has already been used in Eq. (27)] together with (16)–(17), one may write the thrust as

$$T \equiv -D = -\alpha L + T_1 + T_2, \tag{29}$$

with

$$T_1 = \rho\dot\alpha\int_{-1}^1 x\varpi_0\,dx \tag{30}$$

and

$$T_2 = \rho\int_1^\infty[\dot h + a\dot\alpha - \alpha U + \dot\alpha(\sqrt{\xi^2-1}-\xi)]\varpi_e\,d\xi. \tag{31}$$

The first term in Eq. (29) is the projection in the flight direction of the normal force to the plate, also included in the T-G approximation (see Appendix B). The second is an apparent mass term, and the third one is the contribution of the wake to the thrust, in addition to that contained in the first term (associated to L_2). This expression includes the contribution due to the suction at the leading edge, together with all the other contributions to the thrust force coming from the vorticity distributions on the airfoil and the vortex wake.

By using (18)–(21) for an oscillating airfoil and taking the corresponding real parts, the thrust or propulsion coefficient $C_T = T/(\rho U^2/2)$ can be written as

$$C_T = -\Re[\alpha]\,C_L + C_{T_1} + C_{T_2}, \tag{32}$$

where C_L is given in Eq. (A1) in Appendix A,

$$C_{T_1} = \pi a_0 k\sin(\omega t+\phi)[(kh_0)\sin(\omega t) + aka_0\sin(\omega t+\phi) + a_0\cos(\omega t+\phi)] \tag{33}$$

and

$$\begin{aligned}C_{T_2} = 4\,\Re&\left\{a_0e^{i(\omega t+\phi)}\left[1-ik\left(a-\frac{1}{2}\right)\right]-i(kh_0)e^{i\omega t}\right\}\\ &\times\Re\left(C_1(k)\{(kh_0)e^{i\omega t}+[2i+k(a-1)]a_0e^{i(\omega t+\phi)}\}-\frac{\pi}{2}C(k)a_0e^{i(\omega t+\phi)}\right),\end{aligned} \tag{34}$$

where

$$C_1(k) \equiv \frac{\frac{1}{k}e^{-ik}}{iH_0^{(2)}(k)+H_1^{(2)}(k)} \equiv F_1(k) + iG_1(k). \tag{35}$$

Figure 2 compares this new complex function $C_1(k)$ with Theodorsen function $C(k)$.

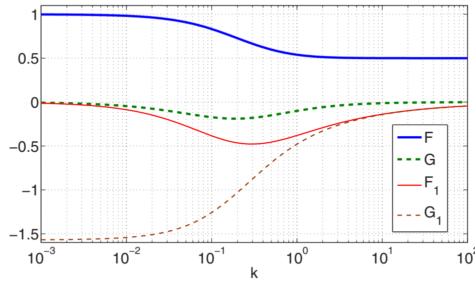

FIG. 2. Theodorsen function $C(k) = F(k) + iG(k)$ (24) and function $C_1(k) = F_1(k) + iG_1(k)$ (35).

It is convenient to define the mean thrust coefficient, or thrust coefficient time-averaged over a cycle of motion:

$$\overline{C}_T = \frac{\omega}{2\pi}\int_t^{t+2\pi/\omega} C_T\, dt. \tag{36}$$

This quantity is given by

$$\begin{aligned}\overline{C}_T &= -2(kh_0)^2 G_1 - a_0^2\{2\pi F + 2akF_1 + 2[2 + k^2(a-1)(a-\tfrac{1}{2})]G_1\}\\ &\quad + a_0(kh_0)\{-[2F_1 + k(4a-3)G_1]\cos\phi + (2\pi F + kF_1 + 6G_1)\sin\phi\}.\end{aligned} \tag{37}$$

In Eq. (37), all the terms coming from C_{T_1} cancel with terms in the other two contributions, so that only part of C_{T_2} and $\Re[\alpha]\, C_L$ contribute to the time-averaged propulsion.

Another quantity of interest is the propulsive efficiency, or ratio of the time-averaged power output of the airfoil and the time-averaged input power required to drive the airfoil:

$$\eta = \frac{\overline{T}U}{\overline{P}} = \frac{\overline{C}_T}{\overline{C}_P}, \tag{38}$$

where the power P and the mean power coefficient $\overline{C}_P$ are defined and given in Eqs. (A3) and (A5), respectively, in Appendix A.

In the next section we shall compare the mean thrust (37) and the thrust efficiency (38) with the corresponding values $\overline{C}_{T_G}$ and $\eta_G = \overline{C}_{T_G}/\overline{C}_P$ given by the T-G theory (see Appendix B). But before that, it is useful to add some comments about the non-dimensional parameters governing the problem. The nondimensional parameters appearing in the above defined coefficients are the pitching amplitude and phase shift, a_0 and ϕ, the pivot point location a, and two Strouhal numbers, one based on the chord length c, which has been written here in terms of the reduced frequency,

$$k = \frac{\omega c}{2U} = \pi \mathrm{St}_c, \quad \mathrm{St}_c = \frac{fc}{U}, \quad f = \frac{\omega}{2\pi}, \tag{39}$$

and the other one based on the plunging amplitude $h_0^* = (c/2)h_0$, related to the nondimensional parameter kh_0,

$$kh_0 = \frac{\omega h_0^*}{U} = 2\pi \mathrm{St}_a = \frac{1}{J}, \quad \mathrm{St}_a = \frac{fh_0^*}{U}, \quad J = \frac{U}{\omega h_0^*}, \tag{40}$$

where J is the advance ratio. It is common in the literature on the aerodynamics of flapping flight to use the couple of nondimensional parameters reduced frequency k and advance ratio J (e.g., Refs. [2,29]), or the two Strouhal numbers St_c and St_a (e.g., Refs. [18,24]). Here we use k and kh_0, which is also a common choice (e.g., Refs. [8,12,30]), serving the relations (39)–(40) to compare different results.

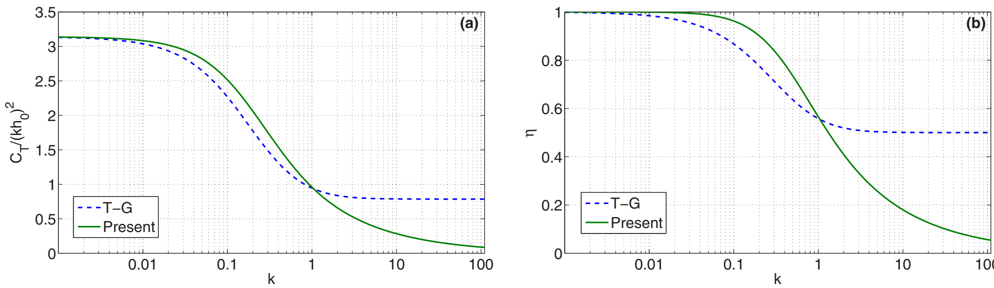

FIG. 3. Comparison of $\overline{C}_T/(kh_0)^2$ (a) and η (b) given by T-G theory (dashed lines) and by the present theory (continuous lines) for pure plunging motion ($a_0 = 0$).

IV. COMPARISON WITH THEODORSEN-GARRICK PROPULSION AND WITH EXPERIMENTAL AND NUMERICAL RESULTS

The expressions (37) and (B4) for the mean propulsion coefficients seem quite different. But, in order to appreciate the main differences, if any, it is convenient to compare them first in some special limits.

A. Pure plunging motion

For pure plunging motion ($a_0 = 0$), the two expressions simplify to

$$\overline{C}_T = -2(kh_0)^2 G_1(k), \quad \overline{C}_{T_G} = \pi (kh_0)^2 [F^2(k) + G^2(k)]. \tag{41}$$

The corresponding propulsive efficiencies are

$$\eta = -\frac{2G_1(k)}{\pi F(k)}, \quad \eta_G = \frac{F^2(k) + G^2(k)}{F(k)}. \tag{42}$$

Figure 3 compares these expressions for a wide range of values of k. Note that neither $\overline{C}_T/(kh_0)^2$ nor η depend on the amplitude h_0 in both theories. It is observed that the results are quite similar for small reduced frequencies, with the the maximum propulsion efficiency unity reached for $k \to 0$, and with both $\overline{C}_T$ and η from the T-G theory slightly larger than from the present results for $k \lesssim 1$. The main differences are, however, for large k, with $\eta_G \to 1/2$ as $k \to \infty$, while $\eta \to 0$ in the present theory for $k \to \infty$, in accordance with experimental and numerical results for pure plunging motions. For instance, the results for the propulsive efficiency obtained by Young and Lai [9,31] with an unsteady panel method and from full Navier-Stokes simulations using a NACA0012 airfoil have the same behavior as the present results for $k \gtrsim 1$ and disagree with the T-G results (Fig. 4).

Actually, both T-G propulsion coefficient $\overline{C}_{T_G}$ and the present $\overline{C}_T$ are in reasonable agreement with experimental data and with full Navier-Stokes simulations for high Reynolds numbers if h_0 is small enough [Fig. 5(a)]: the propulsion coefficient $\overline{C}_{T_G}$ from the T-G theory and that from the unsteady panel method overestimate the experimental data and Navier-Stokes numerical results, while $\overline{C}_T$ from the present theory agree with the experimental data and numerical results in a wide frequencies range. However, the T-G prediction for the propulsive efficiency η is quite bad for large frequencies, since it tends to a constant (1/2), while the efficiency from the present theory correctly predicts its decay for large frequencies, though overestimating the experimental and numerical data just like the results from the unsteady panel method [Fig. 5(b)]. Obviously, the efficiency from the inviscid theories (T-G, present and UPM) are not valid for very low frequencies, since viscous effects are then very important. That is why these theories do not predict the maximum in the propulsive efficiency for a finite Strouhal number found in experiments and full NS numerical simulations for pure plunging motions.

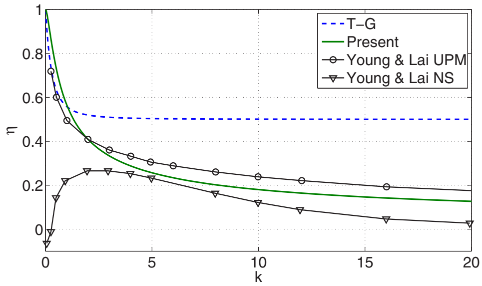

FIG. 4. Propulsive efficiencies vs k given by (42) for pure plunging motion compared with numerical results by Young and Lai [9,31] employing a NACA0012 airfoil with $kh_0 = 0.6$ computed with an unsteady panel method (UPM), and form the full Navier-Stokes (NS) equations with Reynolds number 20 000 and Mach number 0.05 (data from Fig. 6.11 in Ref. [31]).

B. Pure pitching motion

For pure pitching motion ($h_0 = 0$),

$$\overline{C}_T = -a_0^2\{2\pi F + 2akF_1 + 2[2 + k^2(a-1)(a-\tfrac{1}{2})]G_1\}, \tag{43}$$

$$\overline{C}_{T_G} = \pi a_0^2\{[1 + (a-\tfrac{1}{2})^2k^2]|C|^2 + (a-\tfrac{1}{2})(F-\tfrac{1}{2})k^2 - (a+\tfrac{1}{2})kG - F\}, \tag{44}$$

which are compared, together with the corresponding propulsive efficiencies, in Fig. 6 for two values of a: $a = 0$, or pitching motion about the center of the airfoil chord, and $a = -1/3$, pitching about 1/3 chord length from the leading edge. Note that neither $\overline{C}_T/a_0^2$ nor η depend on the amplitude a_0 of the oscillations in both theories. The mean thrust coefficient is negative (it becomes a drag coefficient) for values of the reduced frequency smaller than a value k^* that depends on a [Fig. 6(b)]. For the cases plotted in Fig. 6, k^* is smaller for the T-G theory than for the present results, and for $a = -1/3$ than for $a = 0$ in both cases [$k^* = 1.781$ in the T-G theory for $a = 0$, as reported in Ref. [32], and $k^* = 1.128$ for $a = -1/3$, while $k^* = 2.274$ and 1.601 in the present theory for $a = 0$ and $a = -1/3$, respectively]. It is also observed that $\overline{C}_{T_G} > \overline{C}_T$ and $\eta_G > \eta_G$ for positive thrust ($k > k^*$). But the main qualitative difference between the T-G and the present results is that the T-G propulsive efficiency tends again to a constant (1/2) as $k \to \infty$, while the new propulsive efficiency decays to zero, in accordance with experimental and numerical results. In fact, it decays as k^{-1}, as recently demonstrated theoretically and corroborated with numerical simulations by

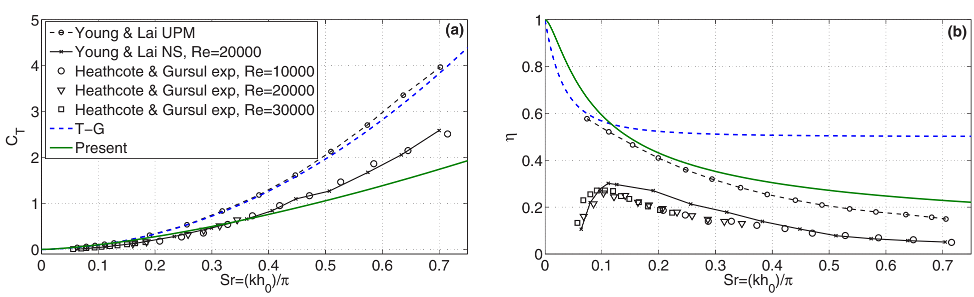

FIG. 5. $\overline{C}_T$ (a) and η (b) vs Strouhal number $\mathrm{Sr} = 2\mathrm{St}_a = (kh_0)/\pi$ for pure plunging motion with $h_0 = 0.35$ compared with numerical results by Young and Lai (see caption of Fig. 4) and experimental results by Heathcote and Gursul [10] for a NACA0012 airfoil with $h_0 = 0.35$ and three values of the Reynolds number (data from Refs. [10,11]).

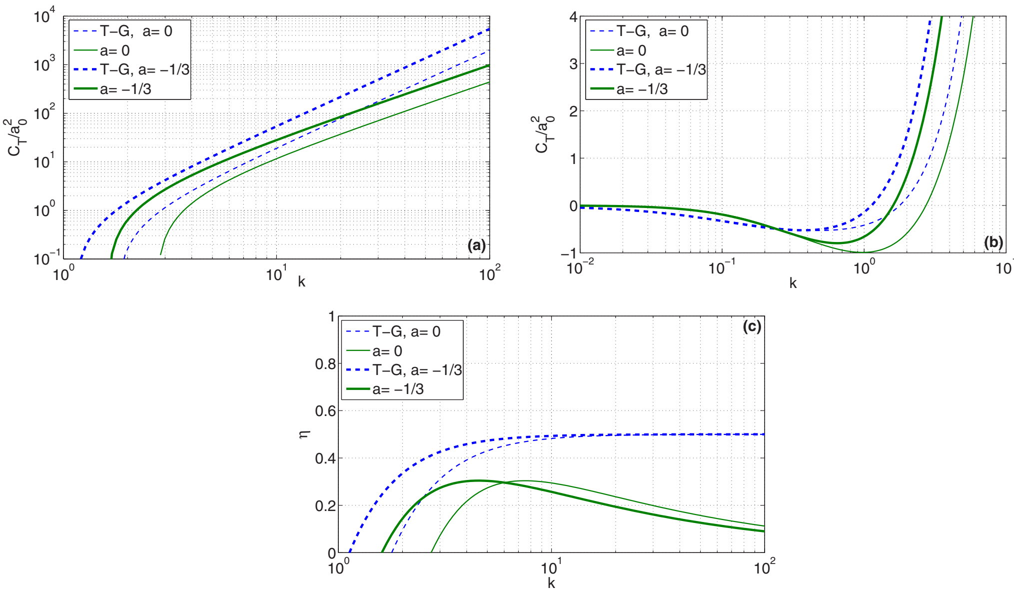

FIG. 6. Comparison of $\overline{C}_T/a_0^2$ (a) and (b) and η (c) given by T-G theory (dashed lines) and by the present theory (continuous lines) for pure pitching motion ($h_0 = 0$) for two values of the pivot parameter a.

Das *et al.* [33] for pure pitching motion. As a difference with the pure plunging motion, η decays to zero as k decreases in both cases, so the present theory correctly predicts that the propulsive efficiency η presents a maximum for a finite value of the reduced frequency that depends on a [Fig. 6(c)].

Figure 7 shows a comparison between the theoretical results with experimental measurements by Mackowski and Williamson [34] and with numerical simulations by Das *et al.* [33] for a NACA 0012 airfoil pitching about its quarter-chord point ($a = -1/2$) with very small amplitudes ($a_0 = 2^\circ$ and 5°). The experimental data and numerical results agree much better with the present theory than with T-G results. Note that the abscissas in Fig. 7(b) is a Strouhal number based on the peak-to-peak trailing edge amplitude A, $\mathrm{St}_A = fA/U = k \times 3a_0/(2\pi)$ for $a = -1/2$.

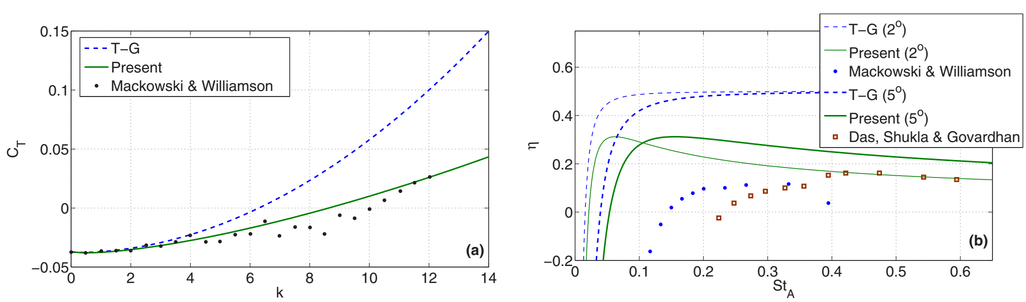

FIG. 7. (a) Comparison of $\overline{C}_T$ vs k given by T-G and by the present theory with experimental data by Mackowski and Williamson [34] for a pitching NACA0012 airfoil with $a = -1/2$ and $a_0 = 2^\circ$ at Re = 16 000. According to Ref. [34], a constant offset representing the viscous, static drag of the airfoil section has been added to the theoretical results to present a more meaningful comparison with measured data. (b) η vs $\mathrm{St}_A = k \times 3a_0/(2\pi)$ given by T-G and by the present theory compared with the same experimental data, and with numerical results by Das *et al.* [33] also for $a = -1/2$, but $a_0 = 5^\circ$ and Re = 2000.

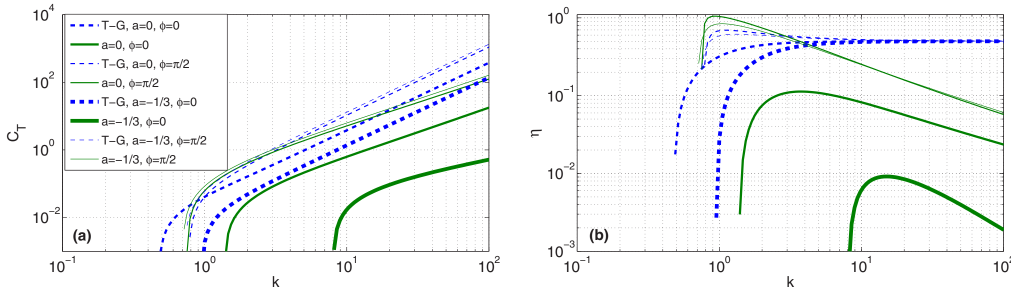

FIG. 8. Comparison of $\overline{C}_T$ (a) and η (b) given by T-G theory (dashed lines) and by the present theory (continuous lines) for combined plunging and pitching motions with $h_0 = 0.35$, $a_0 = 0$ and for two values of the pivot parameter a and two values of the phase shift angle ϕ (as indicated).

C. Combined plunging and pitching motions

For general pitching and plunging motions one has to use the complete expressions (37) and (B4) for the mean propulsion coefficients, and the corresponding ones (divided by the same $\overline{C}_P$) for the propulsive efficiencies. An exhaustive comparison between both results for all the values of the parameters would be too lengthy, so that we just consider here the effect of the pivot parameter a and the phase shift angle ϕ for given values of the plunging and pitching amplitudes h_0 and a_0: $h_0 = 0.35$ and $a_0 = 15^\circ$ (see Fig. 8), which are sufficiently small for the validity of the linearized theory. Two different values of a and ϕ are selected in Fig. 8: $a = 0, -1/3$, and $\phi = 0, \pi/2$.

As in previous cases with pure plunging and pitching motions, the main difference resides in the fact that the T-G propulsive efficiency always tend to $1/2$ for large k, while in the present theory $\eta \to 0$ as $k \to \infty$, in accordance with numerical and experimental results. Thus, the present propulsive efficiency presents a maximum value for a finite reduced frequency that depends on the rest of the nondimensional parameters. In addition, T-G mean thrust and efficiency are, in general, larger than the present results. But, for phase shift $\phi = \pi/2$, there is a region of reduced frequencies around unity where the present mean thrust and efficiency are larger than the corresponding T-G results. This is particularly clear in Fig. 8(b), where a marked maximum of the efficiency is observed at $k \approx 1$ when $\phi = \pi/2$, for the two values of a considered. This enhanced propulsive efficiency around reduced frequency unity in relation to the T-G result is found for $45^\circ \lesssim \phi \lesssim 160^\circ$ for $a = 0$. A formal search for the optimal efficiency as the parameters are varied is, however, out of the scope of the present work.

V. CONCLUSION

The propulsion force and propulsive efficiency obtained analytically in the present work for a plunging and pitching airfoil by using the vortical impulse theory within the framework of the linearized potential theory modifies in a significant way the classical result by Garrick, particularly for reduced frequencies k larger than about unity. It is perhaps surprising that this classical result, that takes into account (in addition to the projection in the direction of flight of the normal forces to the airfoil) only the suction force at the leading edge has not been corrected by considering the complete effect of the nonstationary vortex wake on all the points of the airfoil, not just on its leading edge. Here it is shown that this whole effect correctly predicts the decay of the propulsive efficiency for large reduced frequencies as k^{-1}, and the fact that the efficiency reaches a maximum for a finite value of k, in contrast to Garrick's theory. The results have been favourably compared to experimental data and numerical simulations for the case of pure plunging and pure pitching motions, for which results for airfoil oscillations with small enough amplitudes for the linearized theory to be valid are available.

ACKNOWLEDGMENT

This research has been supported by the Ministerio de Economía y Competitividad of Spain Grant No. DPI2013-40479-P.

APPENDIX A: THEODORSEN LIFT, MOMENT, AND POWER COEFFICIENTS

Taking the real part of (22) and (23) and using (2), (3), (18), and (24), the lift and moment coefficients can be written as

$$C_L \equiv \frac{L}{\frac{1}{2}\rho U^2 c} = 2\pi\Bigg((kh_0)\left\{\left[G(k)+\frac{k}{2}\right]\cos(\omega t)+F(k)\sin(\omega t)\right\} + a_0\left\{\cos(\omega t+\phi)\left[\frac{ak^2}{2}+F(k)+G(k)k\left(a-\frac{1}{2}\right)\right] + \sin(\omega t+\phi)\left[-\frac{k}{2}-G(k)+F(k)k\left(a-\frac{1}{2}\right)\right]\right\}\Bigg), \tag{A1}$$

$$C_M \equiv \frac{M}{\frac{1}{2}\rho U^2 c^2} = \pi\Bigg((kh_0)\left\{\left[G(k)\left(a+\frac{1}{2}\right)+\frac{ak}{2}\right]\cos(\omega t)+F(k)\left(a+\frac{1}{2}\right)\sin(\omega t)\right\} + a_0\left\{\cos(\omega t+\phi)\left[\frac{k^2}{2}\left(a^2+\frac{1}{2}\right)+\left(a+\frac{1}{2}\right)F(k)+\left(a^2-\frac{1}{4}\right)G(k)k\right] + \sin(\omega t+\phi)\left[\frac{k}{2}\left(\frac{1}{2}-a\right)-\left(a+\frac{1}{2}\right)G(k)+\left(a^2-\frac{1}{4}\right)F(k)k\right]\right\}\Bigg), \tag{A2}$$

where $F(k)$ and $G(K)$ are the real and imaginary parts of Theodorsen function (24).

The mean or time-averaged values of both lift and moment vanish. On the other hand, the power required to drive the airfoil motion is

$$P = -\Re[L]\Re[\dot{h}] - \Re[M]\Re[\dot{\alpha}]. \tag{A3}$$

The input power coefficient can be written as

$$C_P = \frac{P}{\frac{1}{2}\rho U^3 c} = -C_L\Re[\dot{h}] - C_M\Re[\dot{\alpha}], \tag{A4}$$

where now the length and time are both scaled with $c/2$ and $c/(2U)$, respectively. Its mean value, time-averaged over one cycle of motion, is

$$\overline{C}_P = \pi(kh_0)^2F + \pi a_0^2\left[\left(a^2-\frac{1}{4}\right)k^2F - \left(a+\frac{1}{2}\right)kG - \frac{1}{2}\left(a-\frac{1}{2}\right)k^2\right] + \pi(kh_0)a_0\left[(-F+kG)\sin\phi + \left(2akF - G - \frac{k}{2}\right)\cos\phi\right]. \tag{A5}$$

APPENDIX B: THEODORSEN-GARRICK PROPULSION

According to Garrick [7], the thrust or propelling force per unit span can be written, in the present notation, as

$$T_G = -D_G = \pi\rho(\Re[S])^2 - \Re[\alpha]\Re[L], \tag{B1}$$

where the subscript G is added to distinguish it from that computed in Sec. III. The first term is the horizontal force due to the leading-edge suction, with

$$S = \lim_{x\to -1} \tfrac{1}{2}\sqrt{x+1}\,\varpi_s, \tag{B2}$$

and the second term is the projection in the flight direction of the normal pressure force on the plate, with L given by (22) (of course valid for small $|\alpha|$).

On using (12), (14), (18), and (19),

$$S = \frac{1}{\sqrt{2}}\left[\frac{\Gamma_0}{\pi} - 2\dot{h} - 2(a+1)\dot{\alpha} + 2U\alpha\right] + \frac{\sqrt{2}}{\pi}\int_1^\infty \frac{\varpi_e}{\sqrt{\xi^2-1}}\,d\xi = \frac{1}{\sqrt{2}}\left[\frac{\Gamma_0}{\pi}C(k) - \dot{\alpha}\right]. \tag{B3}$$

The thrust coefficient time-averaged over a cycle of motion is

$$\begin{aligned}\overline{C}_{T_G} = {}& \pi(kh_0)^2|C|^2 + \pi a_0^2\left\{\left[1+\left(a-\frac{1}{2}\right)^2 k^2\right]|C|^2 + \left(a-\frac{1}{2}\right)\left(F-\frac{1}{2}\right)k^2 - \left(a+\frac{1}{2}\right)kG - F\right\}\\ &+ \pi(kh_0)a_0\left\{(-2|C|^2 + kG + F)\sin\phi + \left[k(2a-1)|C|^2 + kF - G - \frac{k}{2}\right]\cos\phi\right\}.\end{aligned} \tag{B4}$$

---

[1] M. Platzer, K. Jones, J. Young, and J. Lai, Flapping wing aerodynamics: progress and challenges, AIAA J. **46**, 2136 (2008).
[2] W. Shyy, H. Aono, C. K. Kang, and H. Liu, *An Introduction to Flapping Wing Aerodynamics* (Cambridge University Press, Cambridge, 2013).
[3] H. Glauert, The force and moment on an oscillating airfoil, Technical Report R and M-1242, Aeronautical Research Committee (1929).
[4] T. Theodorsen, General theory of aerodynamic instability and the mechanism of flutter, Technical Report TR 496, NACA (1935).
[5] Th. von Kármán and W. R. Sears, Airfoil theory for non-uniform motion, J. Aeronaut. Sci. **5**, 370 (1938).
[6] Th. von Kármán and J. M. Burgers, General aerodynamic theory: Perfect fluids, in *Aerodynamic Theory*, edited by W. F. Durand (Springer, Berlin, 1935), Vol. II, Sec. V.A.9.
[7] I. E. Garrick, Propulsion of a flapping and oscillating airfoil, Technical Report TR 567, NACA (1936).
[8] J. C. S. Lai and M. F. Platzer, Jet characteristics of a plunging airfoil, AIAA J. **37**, 1529 (1999).
[9] J. Young and J. C. S. Lai, Oscillation frequency and amplitude effects on the wake of a plunging airfoil, AIAA J. **42**, 2042 (2004).
[10] S. Heathcote and I. Gursul, Flexible flapping airfoil propulsion at low Reynolds numbers, AIAA J. **45**, 1066 (2007).
[11] J. Young and J. C. S. Lai, Mechanisms influencing the efficiency of oscillating airfoil propulsion, AIAA J. **45**, 1695 (2007).
[12] M. A. Asraf, J. Young, and J. C. S. Lai, Oscillation frequency and amplitude effects on plunging airfoil propulsion and flow periodicity, AIAA J. **50**, 2308 (2012).
[13] J. Lighthill, *An Informal Introduction to Theoretical Fluid Mechanics* (Clarendon Press, Oxford, 1986).
[14] P. G. Saffman, *Vortex Dynamics* (Cambridge University Press, New York, 1992).
[15] J. Z. Wu, H. Y. Ma, and M. D. Zhou, *Vorticity and Vortex Dynamics* (Springer, New York, 2006).
[16] M. H. Dickinson and K. G. Götz, Unsteady aerodynamics performance of model wings at low Reynolds numbers, J. Exp. Biol. **174**, 45 (1993).
[17] C. P. Ellington, C. van den Berg, A. P. Willmott, and A. L. R. Thomas, Leading-edge vortices in insect flight, Nature (London) **384**, 626 (1996).
[18] Z. J. Wang, Vortex shedding and frequency selection in flapping fight, J. Fluid Mech. **410**, 323 (2000).
[19] F. O. Minotti, Unsteady two-dimensional theory of a flapping wing, Phys. Rev. E **66**, 051907 (2002).

[20] T. Maxworthy, The formation and maintenance of a leading-edge vortex during the forward motion of an animal wing, J. Fluid Mech. **587**, 471 (2007).

[21] W. Shyy and H. Liu, Flapping wings and aerodynamic lift: The role of the leading-edge vortex, AIAA J. **45**, 2817 (2007).

[22] Y. S. Baik, L. P. Bernal, K. Granlund, and M. V. Ol, Unsteady force generation and vortex dynamics of pitching and plunging aerofoils, J. Fluid Mech. **709**, 37 (2012).

[23] C. W. Pitt and H. Babinsky, Lift and the leading-edge vortex, J. Fluid Mech. **720**, 280 (2013).

[24] A. Martín-Alcántara, R. Fernandez-Feria, and E. Sanmiguel-Rojas, Vortex flow structures and interactions for the optimum thrust efficiency of a heaving airfoil at different mean angles of attack, Phys. Fluids **27**, 073602 (2015).

[25] J. Li and Z. N. Wu, Unsteady lift for the Wagner problem in the presence of additional leading/edge vortices, J. Fluid Mech. **769**, 182 (2015).

[26] H. Wagner, Uber die Enstehung des dynamischen Auftriebes von Tragflügeln, Z. Angew. Math. Mech. **5**, 17 (1925).

[27] F. W. J. Olver and L. C. Maximon, Bessel functions, in *NIST Handbook of Mathematical Functions*, edited by F. W. J. Olver, D. W. Lozier, R. F. Boisvert, and C. W. Clark (National Institute of Standards and Technology, Washington, DC, 2010), pp. 215–286.

[28] I. E. Garrick, On some reciprocal relations in the theory of nonstationary flows, Technical Report TR 629, NACA (1938).

[29] R. Dudley, *The Biomechanics of Insect Flight* (Princeton University Press, Princeton, 2000).

[30] G. C. Lewin and H. Haj-Hariri, Modelling thrust generation of a two-dimensional heaving airfoil in a viscous flow, J. Fluid Mech. **492**, 339 (2003).

[31] J. Young, Numerical simulation of the unsteady aerodynamics of flapping airfoils, Ph.D. thesis, School of Aerospace, Civil and Mechanical Engineering, University of New South Wales, Camberra, Australia, 2005.

[32] T. Y. Wu, Hydromechanics of swimming propulsion. Part 2. Some optimum shape problems, J. Fluid Mech. **46**, 521 (1971).

[33] A. Das, R. K. Shukla, and R. N. Govardhan, Existence of a sharp transition in the peak propulsive efficiency of a low-Re pitching foil, J. Fluid Mech. **800**, 307 (2016).

[34] A. W. Mackowski and H. K. Williamson, Direct measurement of thrust and efficiency of an airfoil undergoing pure pitching, J. Fluid Mech. **765**, 524 (2015).